Fundamental limits on clock precision from spacetime uncertainty in quantum collapse models

Nicola Bortolotti,[1,2,3,*] Catalina Curceanu,[3,4,†] Lajos Diósi,[5,6] Simone Manti,[3] and Kristian Piscicchia[1,3]

[1]Centro Ricerche Enrico Fermi—Museo Storico della Fisica e Centro Studi e Ricerche "Enrico Fermi", Via Panisperna 89 A, 00184 Rome, Italy

[2]Physics Department, "Sapienza" University of Rome, Piazzale Aldo Moro 5, 00185 Rome, Italy

[3]Laboratori Nazionali di Frascati, Istituto Nazionale di Fisica Nucleare, Via Enrico Fermi 54, 00044 Frascati, Italy

[4]IFIN-HH, Institutul National pentru Fizica si Inginerie Nucleara Horia Hulubei, 30 Reactorului, 077125 Măgurele, Romania

[5]Wigner Research Center for Physics, P.O. Box 49, H-1525 Budapest 114, Hungary

[6]Eötvös Loránd University, Pázmány Péter stny, 1/A, H-1117 Budapest, Hungary

(Received 8 April 2025; accepted 31 July 2025; published 13 November 2025)

Models of spontaneous wavefunction collapse explain the quantum-to-classical transition without invoking the von Neumann measurement postulate. Prominent frameworks, such as the Diósi-Penrose (DP) and continuous spontaneous localization (CSL) models, propose a continuous, spontaneous measurement of the mass density field of quantized matter. We show that this mechanism could link both models—not just DP—to fundamental uncertainties in Newtonian gravity. Despite their nonrelativistic nature, these models suggest an induced uncertainty in the flow of time due to fluctuations in the Newtonian potential. We calculate the ultimate limit on time uncertainty and demonstrate that the resulting clock-time uncertainty remains negligible for all contemporary timekeeping devices, including atomic clocks.

DOI: 10.1103/p6tj-lg8l

I. INTRODUCTION

Despite the remarkable experimental success of quantum mechanics, its standard formulation retains a somewhat ad hoc character. Within this framework, the quantum-to-classical transition is explained through quantum measurements that induce abrupt wavefunction collapses, requiring measurement devices and, in some interpretations, even a human observer [1–4].

The debate over the correct interpretation of quantum mechanics has persisted throughout the last century and remains unresolved. Among the various proposals, spontaneous collapse models (SCMs)—also referred to as dynamical or objective—offer a compelling alternative [5–12]. These models not only provide a consistent interpretation of quantum mechanics that aligns with existing experimental observations, but also predict novel, testable effects that are currently under intense experimental investigation [13].

Models of spontaneous wavefunction collapse assume that quantum measurements occur continuously and everywhere in nature. The associated wavefunction collapses—often referred to as dynamical, spontaneous, or objective—provide an alternative explanation for the quantum-to-classical transition without invoking the standard quantum measurement postulate. The price to pay is the presence of a certain universal irreversibility that modifies the unitary dynamics of the wavefunction.

This irreversibility may stem from the intrinsic uncertainty in the structure of spacetime [14,15]. Over the past decades, two nonrelativistic proposals of SCMs, known as Diósi-Penrose (DP) model [7,8] and continuous spontaneous localization (CSL) model [10], have attracted growing interest. Although these models share several key features, it is commonly believed that the nature of this uncertainty differs, as the DP model explicitly relies on the hypothesis of spacetime fluctuations, whereas CSL does not. Here we point out, for the first time, that CSL too can be related to spacetime uncertainties.

The latency of CSL's gravity-relatedness is of reason. The DP model corresponds to the spontaneous measurement of the mass density field, which assumes the uncertainty of the Newtonian field [7,8] and even generates it [16,17]. In contrast, CSL originated from the Ghirardi-Rimini-Weber (GRW) model [5], which posits that each particle in the universe undergoes spontaneous localization processes, randomly in time and independently of one another. The original version of CSL involved the spontaneous measurement of the number density field, occurring continuously in both space and time, in accordance with the GRW framework. Eventually, the number density was replaced by the mass density to better align with experimental constraints [18], making the GRW collapse rate mass-proportional [19]. However, the stochastic field responsible for irreversibility in CSL has never been connected to gravity.

Both DP and CSL models are nonrelativistic; hence, by spacetime uncertainties we mean a stochastic fluctuating

*Contact author: nicola.bortolotti@uniroma1.it
†Contact author: catalina.curceanu@lnf.infn.it

component of the Newtonian potential. While heuristic extensions of these models toward relativistic regimes are being explored [20–22], a fully relativistic theory is still missing. Recently, a general relativistic postquantum theory of gravity has been proposed [23], though its renormalizability remains an open question [24]. In our work, we explore a different relativistic effect. According to general relativity, an uncertainty in the Newtonian potential leads to an uncertainty in the flow of time. We study for the first time the impact of such an effect on the time measured by clocks, as predicted by both the DP and the CSL models. Our analysis shows that this contribution is negligible for any currently available clock. Therefore, SCMs do not place practical limitations on the present precision of time measurements.

II. SPONTANEOUS COLLAPSE MODELS

Standard quantum mechanics incorporates two incompatible dynamical principles: a linear, deterministic evolution that enables superposition of states and a nonunitary, measurement-induced process responsible for wavefunction reduction. SCMs provide a unified evolution by modifying the standard dynamical equations with an additional nonunitary term, which becomes significant only for sufficiently macroscopic systems, leading to the quantum-to-classical transition. A particularly compelling class of collapse models employs the mass density operator $\hat{\mu}(\boldsymbol{x})$ as the collapse operator, ensuring that large (macroscopic) quantum fluctuations of the mass density are spontaneously suppressed.

In terms of the density operator $\hat{\rho}(t)$, the dynamics of a system under spontaneous collapse follows the Lindblad master equation

$$\frac{d\hat{\rho}}{dt} = -\frac{i}{\hbar}[\hat{H},\hat{\rho}] - \frac{1}{2\hbar^2}\int d^3x d^3y \mathcal{D}(\boldsymbol{x}-\boldsymbol{y})[\hat{\mu}(\boldsymbol{x}),[\hat{\mu}(\boldsymbol{y}),\hat{\rho}]], \quad (1)$$

where $\hat{H}$ is the standard quantum Hamiltonian of the system and $\mathcal{D}$ is the spatial correlation function of spontaneous $\hat{\mu}$ measurements at different locations. This correlation function necessarily includes a characteristic smearing (or cutoff) length σ, which defines the finite spatial resolution of the $\hat{\mu}$ measurements.

It is sometimes convenient to express Eq. (1) in an equivalent form using the smeared mass density operator $\hat{\mu}_\sigma(\boldsymbol{x}) = \int d^3y g_\sigma(\boldsymbol{x}-\boldsymbol{y})\hat{\mu}(\boldsymbol{y}) = (g_\sigma * \hat{\mu})(\boldsymbol{x})$ and a different correlation function D that does not include the smearing, related to $\mathcal{D}$ through $\mathcal{D}(\boldsymbol{x}) = (g_\sigma * D * g_\sigma)(\boldsymbol{x})$. Here, $*$ is the convolution operator and g_σ is a Gaussian function centered at zero with width σ.

Remarkably, the master equation (1) admits an interesting interpretation in terms of spacetime fluctuations. Using Itô calculus, it can be derived from the following stochastic Schrödinger equation:

$$\frac{d}{dt}|\psi_t\rangle = -\frac{i}{\hbar}\left[\hat{H} + \int d^3x \hat{\mu}(\boldsymbol{x})\phi(\boldsymbol{x},t)\right]|\psi_t\rangle, \quad (2)$$

where ϕ is a classical Gaussian white noise field with zero average and correlation

$$\mathbb{E}[\phi(\boldsymbol{x},t)\phi(\boldsymbol{y},t')] = \mathcal{D}(\boldsymbol{x}-\boldsymbol{y})\delta(t-t'). \quad (3)$$

Equation (2) corresponds to the ordinary Schrödinger equation in the presence of a classical stochastic gravitational field, where ϕ plays the role of the Newtonian potential and $\mathcal{D}$ in Eq. (1) is its spatial correlation function.

Among all the possible SCMs, CSL and DP are by far the most extensively studied. In CSL, the noise is defined by the following unsmeared correlation function:

$$D_{\mathrm{CSL}}(\boldsymbol{x}-\boldsymbol{y}) = \frac{\hbar^2\gamma}{m_0^2}\delta(\boldsymbol{x}-\boldsymbol{y}), \quad (4)$$

where m_0 is a reference mass, typically chosen to be the nucleon mass. Thus, CSL is characterized by two parameters: γ, which sets the strength of the collapse process, and the smearing length, usually denoted by r_C. It is also customary to use the parameter $\alpha = r_C^{-2}$ as an alternative to the smearing length. Together, these parameters determine the collapse rate for a microscopic system, given by $\lambda = \gamma/(4\pi\sigma^2)^{3/2}$. The commonly adopted values for the collapse rate and spatial resolution are $\lambda = 10^{-16}\,\mathrm{s}^{-1}$ and $\sigma = 10^{-7}$ m, respectively, as proposed by Ghirardi, Rimini, and Weber [5]. These values are consistent with most phenomenological analyses of the mass-proportional formulation of the CSL [25,26], with the exception of Ref. [27] which excludes σ values smaller than 2×10^{-7} m.

Unlike the CSL, the DP noise strength is set by the Newton gravitational constant G and involves no new parameter. In fact, it is characterized by the following unsmeared correlation function

$$D_{\mathrm{DP}}(\boldsymbol{x}-\boldsymbol{y}) = \frac{\hbar G}{|\boldsymbol{x}-\boldsymbol{y}|}. \quad (5)$$

A commonly used reference value for the smearing length, sometimes denoted by R_0, is $\sigma = 10^{-9}$ m. This is approximately five times larger than the strongest lower bound available to date [26,28–30].

III. TIME UNCERTAINTY

Building on the previous discussion, we assume a gravitational origin for SCMs attributed to a fluctuating component of the Newtonian potential and explore a relativistic effect associated with such models. We emphasize that the following analysis holds even if we are dealing with nonrelativistic SCMs.

In the presence of a classical fluctuating Newtonian field, general relativity requires that time, as well, must exhibit a certain degree of uncertainty. For simplicity, let us assume a flat background spacetime. The fluctuation δt measured by a clock at location $\boldsymbol{x}$ is given by the relation [31]

$$\delta t(\boldsymbol{x},t) = \frac{1}{c^2}\int_0^t \phi(\boldsymbol{x},\tau)d\tau, \quad (6)$$

which is valid in the perturbative regime, where the 00-metric component is expressed as $g_{00}(\boldsymbol{x},t) = 1 + 2\phi(\boldsymbol{x},t)/c^2$. Again, ϕ is characterized by zero average and a correlation

function as given in Eq. (3). It follows that

$$\mathbb{E}[\delta t] = 0, \quad \mathbb{E}[\delta t(\boldsymbol{x}, t)\delta t(\boldsymbol{y}, t)] = \frac{1}{c^4}\mathcal{D}(\boldsymbol{x}-\boldsymbol{y})\,t. \tag{7}$$

In the following, we characterize the resulting uncertainty associated with any measurement of time. What is the time measured by a clock along its worldtube in the presence of the stochastic noise? Assuming the clock occupies a volume $\mathcal{V}$, the measured time is subject to fluctuations determined by averaging, over $\mathcal{V}$, the local expression provided in Eq. (6). The spatial average of the time correlation function writes as $\langle \delta t^2 \rangle_{\mathcal{V}} = \tau t$, where τ sets the strength of the fluctuation. This quantity has the dimension of time and is defined in terms of the smeared correlation function as

$$\tau = \frac{1}{\mathcal{V}^2}\int_{\mathcal{V}} d^3x \int_{\mathcal{V}} d^3y \frac{1}{c^4}\mathcal{D}(\boldsymbol{x}-\boldsymbol{y}). \tag{8}$$

The explicit expression of the smeared correlation function $\mathcal{D}$ for CSL and DP models is obtained from the relation $\mathcal{D}(\boldsymbol{x}) = (g_\sigma * D * g_\sigma)(\boldsymbol{x})$, using Eqs. (4) and (5), respectively. In the case of CSL, the calculation is straightforward and yields

$$\mathcal{D}_{\mathrm{CSL}}(x) = \frac{\hbar^2\lambda}{m_0^2} e^{-x^2/4\sigma^2}, \tag{9}$$

where $x = |\boldsymbol{x}|$. For DP, it is convenient to perform the calculation in Fourier space, where the convolution is easier to compute. One immediately gets the Fourier transform

$$\tilde{\mathcal{D}}(k) = \frac{4\pi\hbar G}{k^2} e^{-\sigma^2 k^2}, \tag{10}$$

from which the smeared spatial correlation function of the gravitational potential is derived as

$$\mathcal{D}_{\mathrm{DP}}(x) = \frac{\hbar G}{x}\mathrm{erf}\Big(\frac{x}{2\sigma}\Big). \tag{11}$$

Equations (9) and (11) show that correlations are strongest over distances smaller than the smearing length σ and decay beyond this scale. Consequently, the fluctuation strength τ, being proportional to the average of $\mathcal{D}(x)$ over the clock volume, is maximized when the clock's spatial extent does not exceed σ. Its maximal value is given by

$$\tau_{\mathrm{CSL}}^{\max} = \frac{\hbar^2\lambda}{m_0^2 c^4}, \tag{12}$$

$$\tau_{\mathrm{DP}}^{\max} = \frac{\hbar G}{\sqrt{\pi}c^4\sigma}, \tag{13}$$

independently of the clock's geometry.

The evaluation of τ can be carried out analytically by choosing, for instance, a spherical shape for the clock. Changing integration variables to $\boldsymbol{\rho} = (\boldsymbol{x}+\boldsymbol{y})/2$ and $\boldsymbol{r} = (\boldsymbol{x}-\boldsymbol{y})/2$, with Jacobian $\det(J) = 8$, Eq. (8) becomes

$$\tau = \frac{8}{(4\pi R^3/3)^2}\int_{\mathcal{B}_R} d^3\rho \int_{\mathcal{R}_\rho} d^3r \frac{1}{c^4}\mathcal{D}(2|\boldsymbol{r}|), \tag{14}$$

where $\mathcal{B}_R$ is the ball of radius R centered at the origin and $\mathcal{R}_\rho$ is the region defined by all $\boldsymbol{r}$ such that both $\boldsymbol{x} = \boldsymbol{\rho}+\boldsymbol{r}$ and $\boldsymbol{y} = \boldsymbol{\rho}-\boldsymbol{r}$ belong to $\mathcal{B}_R$. For $0 \leqslant |\boldsymbol{r}| \leqslant R-\rho$, this region reduces to $\mathcal{B}_{R-\rho}$, while for $R-\rho \leqslant |\boldsymbol{r}| \leqslant \sqrt{R^2-\rho^2}$ it is a spherical segment defined by

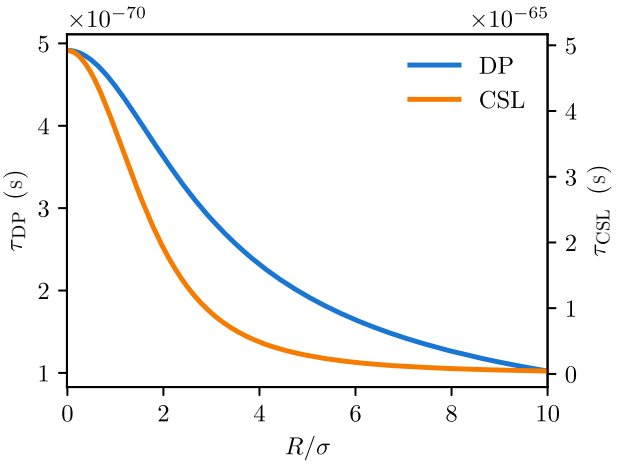

FIG. 1. Time fluctuation strength as a function of the ratio between the clock's radius and the smearing length. The DP case (blue) is plotted on the left axis, and the CSL case (orange) is plotted on the right axis. The smearing length and the collapse rate parameters are set to the standard values: $\lambda = 10^{-16}\,\mathrm{s}^{-1}$, $\sigma_{\mathrm{CSL}} = 10^{-7}\,\mathrm{m}$, and $\sigma_{\mathrm{DP}} = 10^{-9}\,\mathrm{m}$.

$|\hat{\boldsymbol{r}}\cdot\hat{\boldsymbol{\rho}}| = |\cos\theta| \leqslant (R^2-\rho^2-r^2)/(2\rho r)$, corresponding to either $\boldsymbol{x}$ or $\boldsymbol{y}$ lying on the boundary $\partial\mathcal{B}_R$. Thus,

$$\int_{\mathcal{R}} d^3r\mathcal{D}(2|\boldsymbol{r}|) = 4\pi\int_0^{R-\rho} dr r^2\mathcal{D}(2r) + 2\pi\int_{R-\rho}^{\sqrt{R^2-\rho^2}} dr r\frac{R^2-\rho^2-r^2}{\rho}\mathcal{D}(2r). \tag{15}$$

The exact results are shown in Fig. 1 for a specific range of the clock radius R and a choice of parameters corresponding to the standard reference values. Since the smeared correlation function $\mathcal{D}(|\boldsymbol{x}-\boldsymbol{y}|)$ depends only on $|\boldsymbol{x}-\boldsymbol{y}|/\sigma$, a rescaling of the integration variables in Eq. (8) or Eq. (14) shows that τ depends on R through the ratio R/σ. For both CSL and DP, the fluctuation in time measurement is maximal for clock sizes comparable to or smaller than the smearing length σ. In contrast, larger clocks become less sensitive to the uncertainty of spacetime as R increases, leading to more precise measurements of the mean time. This is because the clock measures the mean time within the section $\mathcal{V}$ of its worldtube. The optimal spatial resolution corresponds to the smallest size of $\mathcal{V}$, when timekeeping has the worst precision. Conversely, as $\mathcal{V}$ increases, timekeeping precision improves at the expense of spatial resolution. The asymptotic behavior of the fluctuation strength is as follows:

$$\tau_{\mathrm{CSL}} \sim \tau_{\mathrm{CSL}}^{\max}, \tag{16}$$

$$\tau_{\mathrm{DP}} \sim \tau_{\mathrm{DP}}^{\max}, \tag{17}$$

for $R \lesssim \sigma$ and

$$\tau_{\mathrm{CSL}} \sim \frac{6\sqrt{\pi}\tau_{\mathrm{CSL}}^{\max}}{(R/\sigma)^3}, \tag{18}$$

$$\tau_{\mathrm{DP}} \sim \frac{6\sqrt{\pi}\tau_{\mathrm{DP}}^{\max}}{5(R/\sigma)}, \tag{19}$$

for $R \gg \sigma$.

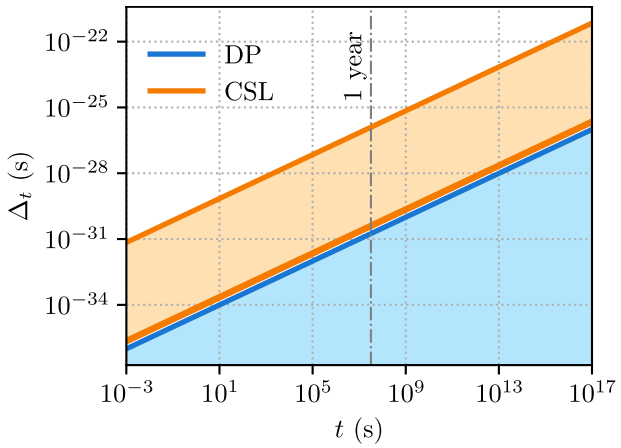

FIG. 2. Time uncertainty for optimal clocks as a function of time, extending up to the age of the universe. The colored areas correspond to the experimentally allowed regions. The blue region encompasses all allowed values constrained by the lower bound on the DP smearing length, $\sigma_{\rm DP} = 4.94 \times 10^{-10}$ m. The orange region corresponds to the range permitted by experimental bounds on the CSL collapse rate, 10^{-20} s$^{-1} < \lambda < 10^{-11}$ s^{-1}. The upper edges of both regions represent the maximum time uncertainty predicted by the DP and CSL models.

In conclusion, the relativistic relation (6) combined with the presence of a stochastic component in the gravitational field implies an unavoidable uncertainty in any time measurement. Regardless of how small τ may be, if it is nonzero, this uncertainty inevitably increases over time. Therefore, it is essential to consider whether this uncertainty could lead to measurable effects, potentially imposing a fundamental limit on clock precision.

After a period of time t, the random component of the gravitational field induces a fluctuation in the measured time given by $\Delta_t = \sqrt{\langle \delta t^2 \rangle_{\mathcal{V}}} = \sqrt{\tau t}$. We focus on optimal clocks with respect to spatial resolution, defined as those with dimensions comparable to the smearing length, for which the fluctuation strength reaches its maximum value $\tau^{\max}$ [Eqs. (12) and (13)]. To provide insight into the relevant orders of magnitude, we set the collapse parameters to their reference values and find, at $t = 1$ year, the values

$$\Delta_t \simeq \begin{cases} 10^{-28} \text{ s in 1 year for CSL,} \\ 10^{-31} \text{ s in 1 year for DP.} \end{cases} \tag{20}$$

For the CSL case, the fluctuation strength is proportional to the microscopic collapse rate. Current experimental constraints on this parameter, reported in Ref. [26], are approximately given by 10^{-20} s$^{-1} < \lambda < 10^{-11}$ s^{-1}. Correspondingly, for these values, the time fluctuation Δ_t at $t =$ 1 year ranges from 10^{-31} to 10^{-26} s. On the other hand, for what regards the DP model, $\tau^{\max}$ is inversely proportional to the smearing length. Experimental bounds place a lower limit on the latter at 4.94×10^{-10} m [26]. Figure 2 shows the uncertainty affecting optimal clocks corresponding to all the experimentally allowed values of the CSL and DP parameters, from which one can see the maximum uncertainties predicted by the CSL and DP models.

We now compare these results with the highest precision achieved by modern clocks. All timekeeping devices operate referencing a stable oscillatory phenomenon, whether it is the swing of a pendulum, the periodic motion of celestial bodies, or the vibration of a quartz crystal. Fluctuations in time measurements due to noise processes are then quantified by the fractional stability $\sigma_y(t)$, which characterizes the frequency stability of the clock over a given period t. The corresponding fluctuation in the measured time is given by $\Delta_t = \sigma_y(t)t/\sqrt{3}$.

Atomic clocks—and potentially future nuclear clocks [32]—are the most precise devices, relying on the exceptional frequency stability of the electromagnetic radiation emitted during atomic transitions. Among these, optically trapped neutral-atom clocks currently set the benchmark for frequency stability, leveraging large ensembles of atoms to reduce statistical noise beyond the limits of single-ion clocks [33]. State-of-the-art optical lattice clocks based on strontium or ytterbium atoms achieve short-term fractional frequency stabilities on the order of $10^{-17}/\sqrt{t/1\,\text{s}}$ [34–36], corresponding to time fluctuations of approximately $10^{-17}\text{s} \cdot \sqrt{t/1\,\text{s}}$ over periods of hours or days.

Over longer time intervals (years or decades), clocks based on millisecond pulsars can approach frequency stabilities comparable to those of atomic clocks [37–39]. However, pulsar clocks are expected to be insensitive to noise induced by SCMs, as this would be suppressed by the extremely small ratio σ/R. Consequently, they could serve as a tool for measuring this type of uncertainty in atomic clocks.

Nevertheless, given these capabilities, it is evident that the uncertainty associated with SCMs is entirely negligible compared to the performance of current timekeeping technology.

IV. CONCLUDING REMARKS

In this article, we addressed the implications of spacetime uncertainty within the context of spontaneous collapse models, focusing on their mass-proportional versions. In this class of models, which includes the leading CSL and DP proposals, the wavefunction collapse dynamics can be attributed to the continuous and spontaneous monitoring of the mass density operator.

We highlighted that the stochastic field defining these models can be interpreted as the Newtonian gravitational potential, possibly relating this class of models to gravity. As a direct consequence, fluctuations in the gravitational field induce an intrinsic uncertainty in the flow of time. We emphasize that while our analyses rely on nonrelativistic collapse models, this effect is fundamentally relativistic in nature. For the first time, we investigated the impact of this time uncertainty on clock measurements. Our results reveal that the effect is maximized for clocks with sizes comparable to the spatial resolution of the collapse (the smearing length σ), while for larger clocks the fluctuations average out, enabling them to measure mean time with higher precision—at the price of lower spatial resolution. Moreover, irrespective of the fluctuation strength, the uncertainty grows unavoidably over time.

We conclude that while spontaneous collapse models introduce a fundamental source of time uncertainty, they do not impose any practical limitation on precision timekeeping. Our findings offer a different perspective on the interplay between

quantum collapse models and gravitational effects, paving the way for further exploration of their possible observational signatures.

ACKNOWLEDGMENTS

This publication was made possible through the support of Grant No. 62099 from the John Templeton Foundation. The opinions expressed in this publication are those of the authors and do not necessarily reflect the views of the John Templeton Foundation. We acknowledge support from the Foundational Questions Institute and Fetzer Franklin Fund, a donor advised fund of Silicon Valley Community Foundation (Grants No. FQXi-RFP-CPW-2008 and No. FQXi-MGB-2011), and from the INFN (VIP). L.D. was supported by the National Research, Development and Innovation Office "Frontline" Research Excellence Program (Grant No. KKP133827). C.C. and L.D. benefited from the EU COST Actions CA23115 and CA23130. N.B. and K.P. acknowledge support from the Centro Ricerche Enrico Fermi—Museo Storico della Fisica e Centro Studi e Ricerche "Enrico Fermi" (Open Problems in Quantum Mechanics project).

DATA AVAILABILITY

No data were created or analyzed in this study.

[1] E. P. Wigner, Remarks on the mind-body question, *Philosophical Reflections and Syntheses* (Springer, Berlin, Heidelberg, 1995), pp. 247–260.

[2] F. London and E. Bauer, The theory of observation in quantum mechanics, *Quantum Theory and Measurement* (Princeton University Press, 1983), pp. 217–259.

[3] H. P. Stapp, Mind, matter, and quantum mechanics, Found. Phys. **12**, 363 (1982).

[4] D. J. Chalmers and K. J. McQueen, Consciousness and the collapse of the wave function, in *Consciousness and Quantum Mechanics*, edited by S. Gao (Oxford University Press, Oxford, 2022).

[5] G. C. Ghirardi, A. Rimini, and T. Weber, Unified dynamics for microscopic and macroscopic systems, Phys. Rev. D **34**, 470 (1986).

[6] P. Pearle, Combining stochastic dynamical state-vector reduction with spontaneous localization, Phys. Rev. A **39**, 2277 (1989).

[7] L. Diósi, Models for universal reduction of macroscopic quantum fluctuations, Phys. Rev. A **40**, 1165 (1989).

[8] L. Diosi, A universal master equation for the gravitational violation of quantum mechanics, Phys. Lett. A **120**, 377 (1987).

[9] G. Ghirardi, R. Grassi, and A. Rimini, Continuous-spontaneous-reduction model involving gravity, Phys. Rev. A **42**, 1057 (1990).

[10] G. C. Ghirardi, P. Pearle, and A. Rimini, Markov processes in Hilbert space and continuous spontaneous localization of systems of identical particles, Phys. Rev. A **42**, 78 (1990).

[11] R. Penrose, On gravity's role in quantum state reduction, Gen. Relativ. Gravit. **28**, 581 (1996).

[12] A. Bassi, K. Lochan, S. Satin, T. P. Singh, and H. Ulbricht, Models of wave-function collapse, underlying theories, and experimental tests, Rev. Mod. Phys. **85**, 471 (2013).

[13] M. Carlesso, S. Donadi, L. Ferialdi, M. Paternostro, H. Ulbricht, and A. Bassi, Present status and future challenges of non-interferometric tests of collapse models, Nat. Phys. **18**, 243 (2022).

[14] F. Karolyhazy, Gravitation and quantum mechanics of macroscopic objects, Nuov. Cim. **42**, 390 (1966).

[15] L. Diósi, Fundamental irreversibility: Planckian or Schrödinger-Newton? Entropy **20**, 496 (2018).

[16] A. Tilloy and L. Diósi, Sourcing semiclassical gravity from spontaneously localized quantum matter, Phys. Rev. D **93**, 024026 (2016).

[17] A. Tilloy and L. Diósi, Principle of least decoherence for Newtonian semiclassical gravity, Phys. Rev. D **96**, 104045 (2017).

[18] K. Piscicchia, A. Bassi, C. Curceanu, R. Del Grande, S. Donadi, B. C. Hiesmayr, and A. Pichler, CSL collapse model mapped with the spontaneous radiation, Entropy **19**, 319 (2017).

[19] P. Pearle and E. Squires, Bound state excitation, nucleon decay experiments and models of wave function collapse, Phys. Rev. Lett. **73**, 1 (1994).

[20] L. Diósi, Relativistic theory for continuous measurement of quantum fields, Phys. Rev. A **42**, 5086 (1990).

[21] G. Ghirardi, R. Grassi, and P. Pearle, Relativistic dynamical reduction models: general framework and examples, Found. Phys. **20**, 1271 (1990).

[22] P. Pearle, Relativistic collapse model with tachyonic features, Phys. Rev. A **59**, 80 (1999).

[23] J. Oppenheim, A postquantum theory of classical gravity? Phys. Rev. X **13**, 041040 (2023).

[24] L. Diósi, Classical-quantum hybrid canonical dynamics and its difficulties with special and general relativity, Phys. Rev. D **110**, 084052 (2024).

[25] S. Donadi, K. Piscicchia, R. Del Grande, C. Curceanu, M. Laubenstein, and A. Bassi, Novel CSL bounds from the noise-induced radiation emission from atoms, Eur. Phys. J. C **81**, 773 (2021).

[26] I. Arnquist *et al.* (MAJORANA Collaboration), Search for spontaneous radiation from wave function collapse in the MAJORANA DEMONSTRATOR, Phys. Rev. Lett. **129**, 080401 (2022).

[27] K. Piscicchia, A. Porcelli, A. Bassi, M. Bazzi, M. Bragadireanu, M. Cargnelli, A. Clozza, L. De Paolis, R. Del Grande, M. Derakhshani *et al.*, A novel approach to parameter determination of the continuous spontaneous localization collapse model, Entropy **25**, 295 (2023).

[28] B. Helou, B. J. J. Slagmolen, D. E. McClelland, and Y. Chen, LISA pathfinder appreciably constrains collapse models, Phys. Rev. D **95**, 084054 (2017).

[29] S. Donadi, K. Piscicchia, C. Curceanu, L. Diósi, M. Laubenstein, and A. Bassi, Underground test of gravity-related wave function collapse, Nat. Phys. **17**, 74 (2021).

[30] S. L. Adler, A. Bassi, M. Carlesso, and A. Vinante, Testing continuous spontaneous localization with Fermi liquids, Phys. Rev. D **99**, 103001 (2019).

[31] L. Diósi, Intrinsic time-uncertainties and decoherence: Comparison of 4 models, Braz. J. Phys. **35**, 260 (2005).

[32] C. Zhang, T. Ooi, J. S. Higgins, J. F. Doyle, L. von der Wense, K. Beeks, A. Leitner, G. A. Kazakov, P. Li, P. G. Thirolf *et al.*, Frequency ratio of the ^{229m}Th nuclear isomeric transition and the ^{87}Sr atomic clock, Nature (London) **633**, 63 (2024).

[33] H. N. Hausser, J. Keller, T. Nordmann, N. M. Bhatt, J. Kiethe, H. Liu, I. M. Richter, M. von Boehn, J. Rahm, S. Weyers, E. Benkler, B. Lipphardt, S. Dörscher, K. Stahl, J. Klose, C. Lisdat, M. Filzinger, N. Huntemann, E. Peik, and T. E. Mehlstäubler, $^{115}In^{+}$ - $^{172}Yb^{+}$ coulomb crystal clock with 2.5×10^{-18} systematic uncertainty, Phys. Rev. Lett. **134**, 023201 (2025).

[34] E. Oelker, R. Hutson, C. Kennedy, L. Sonderhouse, T. Bothwell, A. Goban, D. Kedar, C. Sanner, J. Robinson, G. Marti *et al.*, Demonstration of 4.8×10^{-17} stability at 1 s for two independent optical clocks, Nat. Photon. **13**, 714 (2019).

[35] M. Schioppo, R. C. Brown, W. F. McGrew, N. Hinkley, R. J. Fasano, K. Beloy, T. Yoon, G. Milani, D. Nicolodi, J. Sherman *et al.*, Ultrastable optical clock with two cold-atom ensembles, Nat. Photon. **11**, 48 (2017).

[36] T. Bothwell, C. J. Kennedy, A. Aeppli, D. Kedar, J. M. Robinson, E. Oelker, A. Staron, and J. Ye, Resolving the gravitational redshift across a millimetre-scale atomic sample, Nature (London) **602**, 420 (2022).

[37] G. Hobbs, L. Guo, R. Caballero, W. Coles, K. Lee, R. Manchester, D. Reardon, D. Matsakis, M. Tong, Z. Arzoumanian *et al.*, A pulsar-based time-scale from the International Pulsar Timing Array, Mon. Not. R. Astron. Soc. **491**, 5951 (2020).

[38] A. Rodin and V. Fedorova, Generalized three-cornered hat method and its application for the construction of an ensemble pulsar time scale, Astron. Lett. **48**, 321 (2022).

[39] Y. Dong-shan, G. Yu-ping, and Z. Shu-hong, Ensemble pulsar time scale, Chin. Astron. Astrophys. **41**, 430 (2017).